Investigating the shape of the Milky Way Dark Matter halo with hypervelocity stars in view of future astrometric missions

Arianna Gallo

Turin, May 26, 2020

Supervisor: Dr. Luisa Ostorero

Outline

Project aim: Estimating the precision needed by future astrometric missions to distinguish between different Milky Way dark matter halo shapes.

Tool: Hypervelocity stars (HVSs).

Method: Numerical simulations of HVS kinematics in dark matter halos with different shapes.

- Introduction
- The project
- Next steps

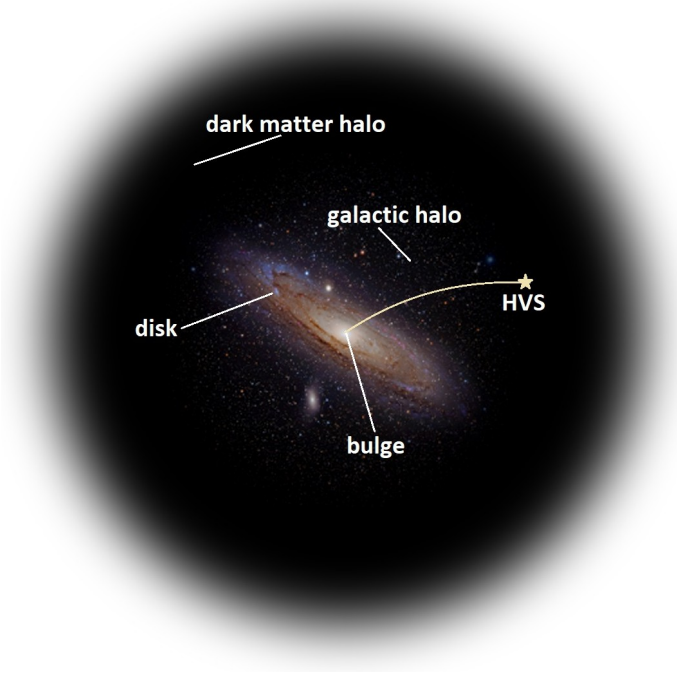

Milky Way dark matter halo

Flat rotation curves of spiral galaxies like the Milky Way (MW) (Rubin & Ford 1970):

→ deviation from the velocity profile expected from the distribution of visible matter;

→ evidence of unseen surrounding matter.

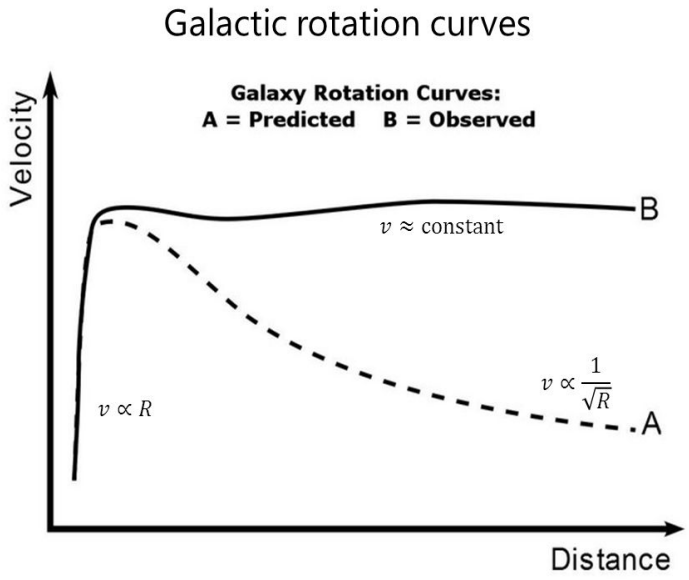

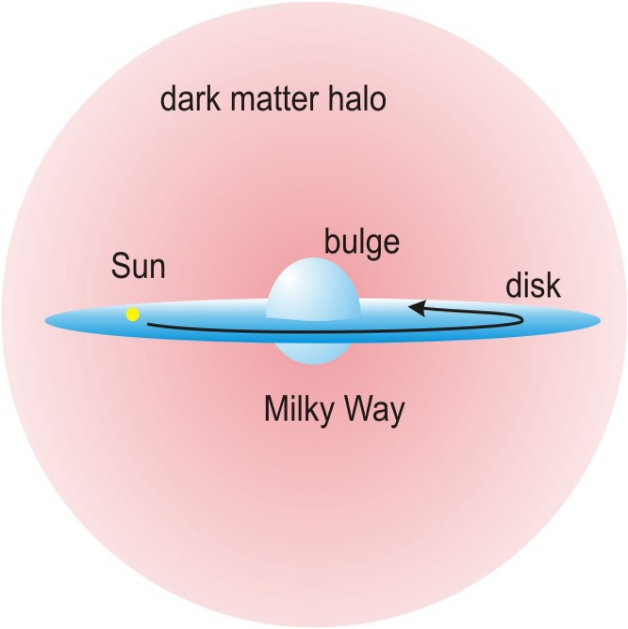

A dark matter (DM) halo can reproduce the asymptotic behavior of the rotation curves of disc galaxies (Ostriker & Peebles, 1973).

Milky Way dark matter halo

ΛCDM scenario: existence of DM halos surrounding the MW and the external galaxies.

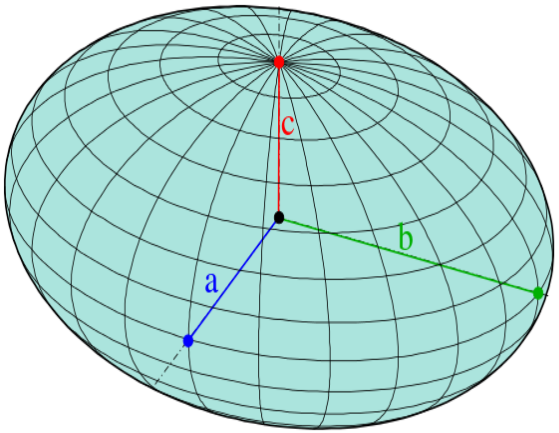

triaxial: $\mathbf{a \neq b \neq c}$

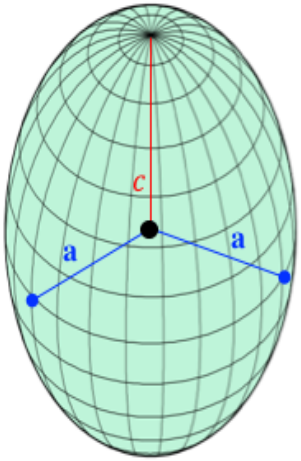

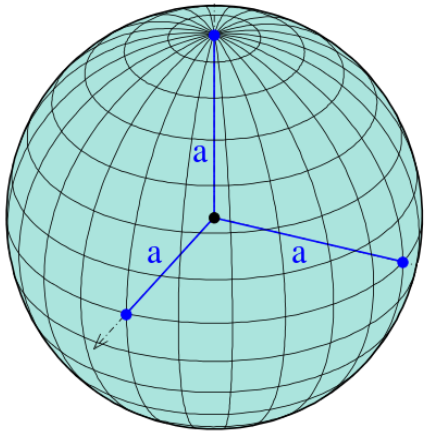

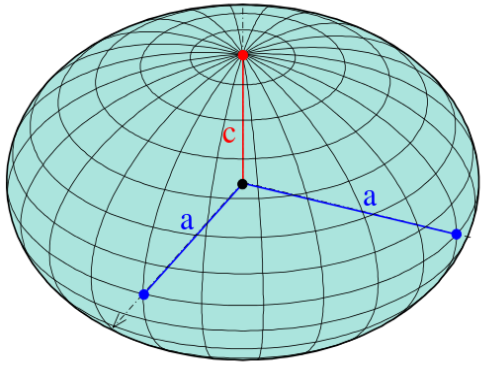

prolate: $\mathbf{a = b < c}$ **sphere: $\mathbf{a = b = c}$** **oblate: $\mathbf{a = b > c}$**

Milky Way dark matter halo

Numerical simulations

- Collisionless N-body simulations: triaxial or near-prolate halos. (e.g., Vera-Ciro et al. 2011)
- Hydro-dynamical simulations: baryonic dissipation changes the shape of DM halos.

  → round or oblate at the center, triaxial at intermediate radii, and prolate at large radii (e.g., Zemp et al. 2012).

Observations

Halo stars and tidal streams as tracers of the Milky Way DM halo mass profile:

- Spherical (Ibata et al. 2001)
- Oblate (Loebman et al. 2014)
- Prolate (Helmi 2004)
- Triaxial (Law & Majewski 2010)

Review: I. De Martino, S. S. Chakrabarty, V. Cesare, **AG**, L. Ostorero, A. Diaferio, 2020 (in press)

Hypervelocity stars

The existence of HVSs was:

- predicted by Hills (1988)
  1) super-massive black hole (SMBH) ejection origin;
  2) $v > v_{\text{escape}}$;
- confirmed by Brown (2005)

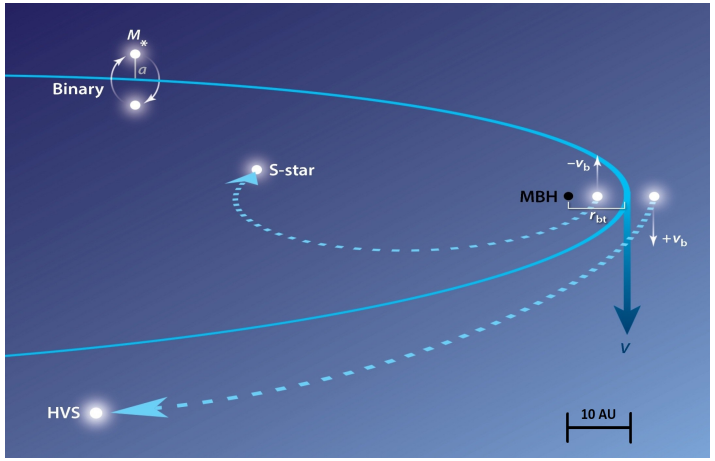

Current sample: ~ 20 HVSs;
$\rightarrow$ heliocentric radial velocity in the range $\sim 200 - 1000$ km/s;
$\rightarrow$ distance from the Sun in the range $\sim 10 - 100$ kpc.

(Gnedin et al., 2005; Fragione & Loeb, 2017; Contigiani et al., 2019)

$\Rightarrow$ Statistical approach: investigate the constraining power of a sample of HVSs on the MW DM halo shape.

Astrometric missions

Relevance of HVS high-precision proper motions to put constraints on the DM halo shape:

- Boehm et al. 2017: proposal for an ESA medium size mission (*Theia*).
- Malbet et al. 2019: white paper for the next planning cycle of the ESA Science Programme.

  → *Gaia* proper motion precision: $40 - 150\ \mu$as/yr;

Proper motion

Apparent motion of a star on the plane of the sky.

$$\mu \left[\frac{\text{as}}{\text{yr}}\right] = \dot{\theta} = 4.74\ \frac{\text{v}_{\text{tan}}\ [\text{km/s}]}{\text{d}\ [\text{pc}]}$$

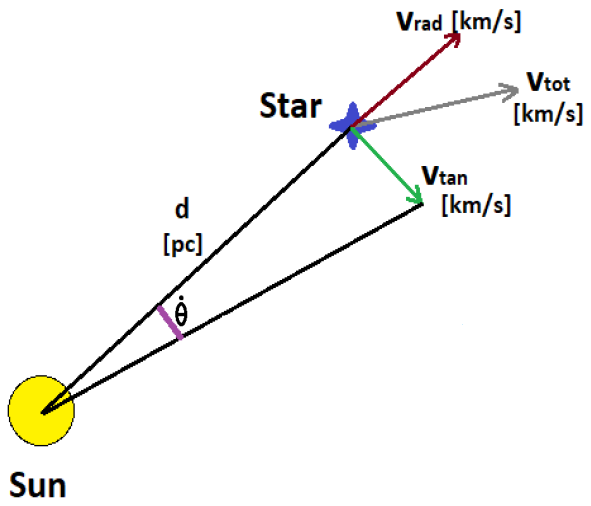

proper motion + radial velocity → star 3D velocity

A numerical code for HVSs trajectories

1) Generation of the initial **distribution of ejection velocities** according to the Hills mechanism;

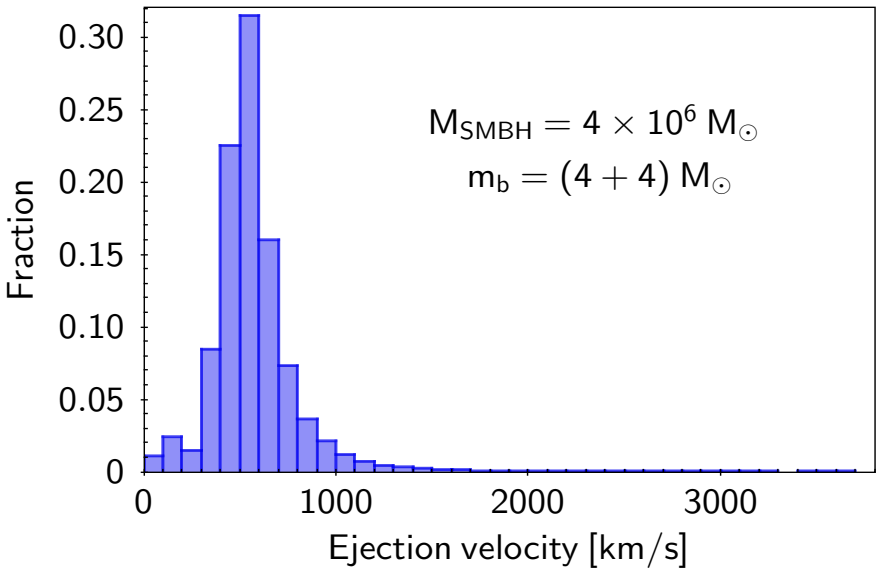

Starting point for the orbit integration:

$r_{\rm influence} = 3$ pc (Genzel et al. 2010)

S. Ebagezio, L. Ostorero, **AG**, (in prep.)

2) computation of the **travel time** of each star;

$$\mathbf{t_{age} + t_{travel} < t_{ms}}$$
$$(m_* = 4\,M_\odot \rightarrow t_{ms} = 160\ \text{Myr})$$

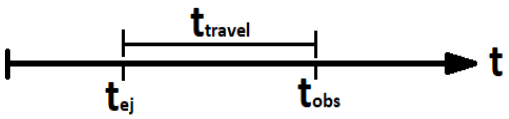

A numerical code for HVSs trajectories

3) integration of the orbit of each star through the solution of the equations of motion in a given **gravitational potential**, described as the superposition of the following components:

- the SMBH: $\Phi_{BH}(r_{GC}) = -\dfrac{G\,M_{BH}}{r_{GC}}$,
- the bulge (Hernquist 1990): $\Phi_b(r_{GC}) = -\dfrac{G\,M_b}{r_{GC} + r_b}$,
- the disk (Miyamoto & Nagai 1975):

$$\Phi_d(R_{GC}, z_{GC}) = -\frac{G\,M_d}{\sqrt{R_{GC}^2 + \left(a_d + \sqrt{z_{GC}^2 + b_d^2}\right)^2}},$$

A numerical code for HVSs trajectories

- the DM halo (Navarro et al. 1996, Vogelsberger et al. 2008):

$$\Phi_h(\tilde{r}) = -\frac{G\,M_{200}}{f(C_{200})}\,\frac{\ln\left(1+\frac{\tilde{r}}{r_s}\right)}{\tilde{r}}, \qquad \tilde{r} = \frac{(r_a + r_{GC})\,r_E}{r_a + r_E},$$

$$r_E = \sqrt{\frac{x^2}{a^2} + \frac{y^2}{b^2} + \frac{z^2}{c^2}}, \qquad f(x) = \ln(1+x) - \frac{x}{(1+x)}$$

$$a^2 + b^2 + c^2 = 3;$$

$$q_y = b/a;$$

$$q_z = c/a.$$

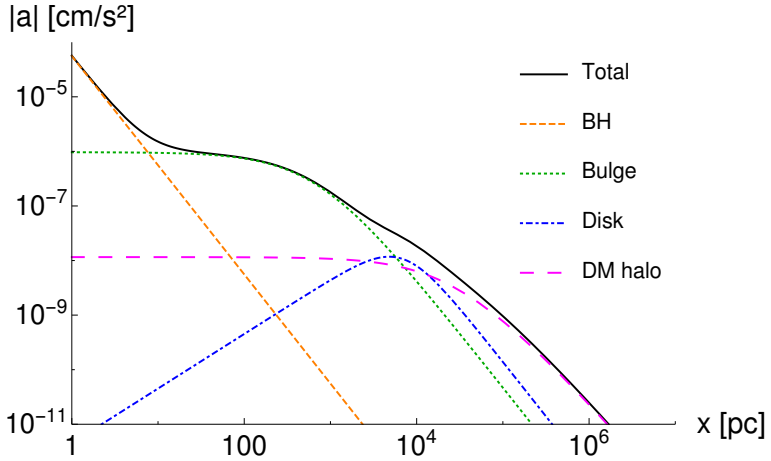

AG et al. (in prep.)

A numerical code for HVSs trajectories

4) generation of **HVS mock catalogs**.

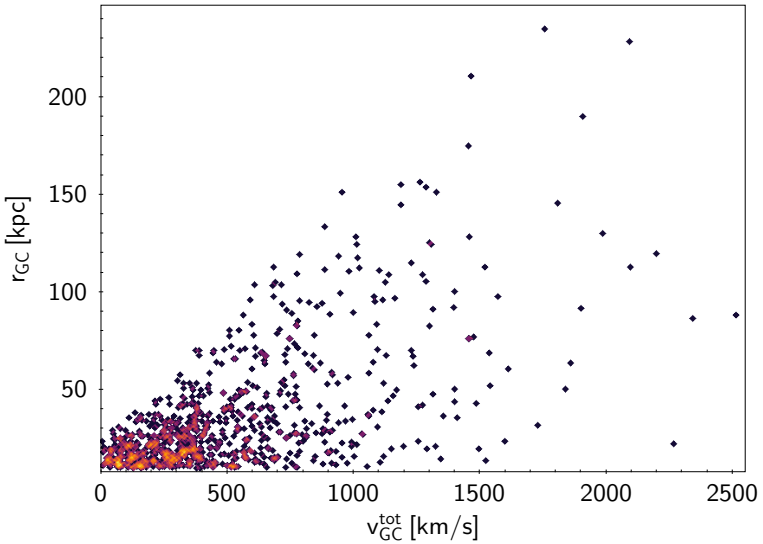

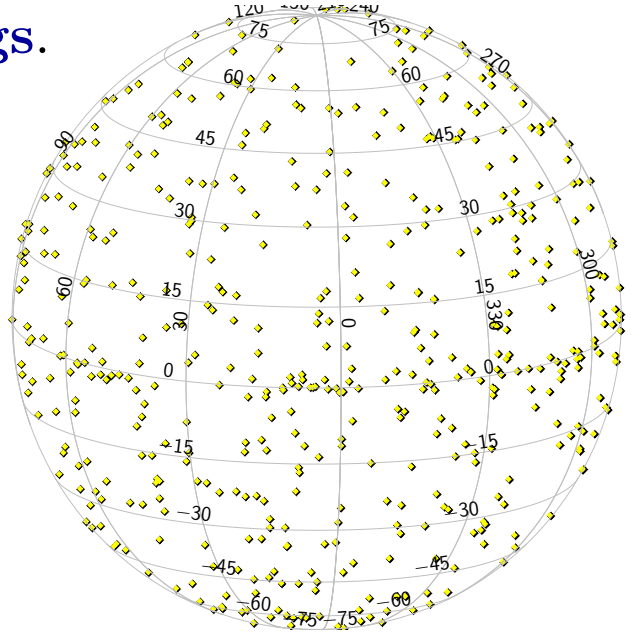

	Galactocentric reference frame							Heliocentric reference frame						
	r [kpc]	θ [°]	φ [°]	v_{rad} [km/s]	v_{tan} [km/s]	v_{tot} [km/s]		d [kpc]	b [°]	l [°]	v_d [km/s]	μ_l [mas/yr]	μ_b [mas/yr]	
#1	14.21	3.81	170.95	384.20	28.72	385.28	[...]	6.48	8.38	159.63	297.35	10.14	-1.77	[...]
#2	19.92	-17.13	324.32	351.64	20.30	352.23		26.61	-12.74	334.68	441.69	-2.30	0.05	
#3	68.59	24.78	290.49	810.07	3.75	810.07		71.53	23.70	297.06	999.63	-0.61	-0.23	
#4	38.75	-2.97	295.83	491.69	12.43	491.85		42.84	-2.68	305.52	679.67	-1.16	0.06	
[...]														

AG et al. (in prep.)

Statistical analysis

AG et al., (in prep.)

- spheroidal DM halo: $q_y = 1$, $q_z = [0.7 - 1.4]$;
- generation of mock catalogs for $q_z = 0.7,\ 1,\ 1.4$;
- two sample **K-S test**: spherical Vs. oblate (prolate);

positions & velocities,
cartesian & spherical coordinates
galactocentric & heliocentric
reference frame.

- Galactocentric tangential velocity: $\mathrm{p-value} < 5\%$

  $\Rightarrow$ key variable to distinguish a spherical DM halo from an oblate (prolate) halo.

Statistical analysis

Spherical-oblate:
$p - \text{value} \sim 10^{-13}$

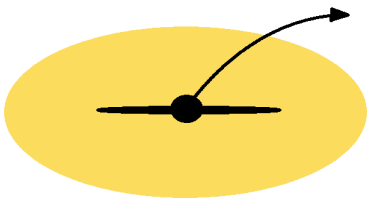

Spherical-prolate:
$p - \text{value} \sim 10^{-14}$

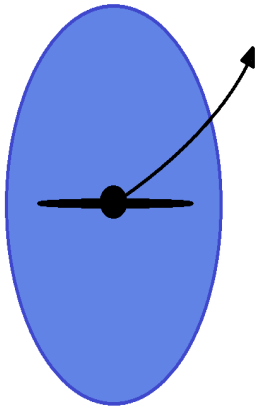

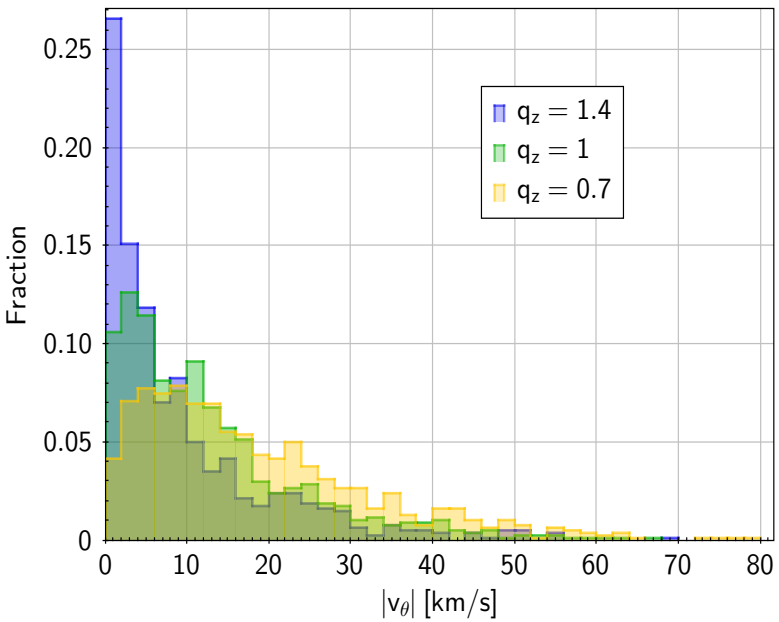

Galactocentric tangential velocity distribution in the prolate (blue), spherical (green), and oblate (yellow) DM halo case.

AG et al. (in prep.)

Statistical analysis

- The **initial conditions** (i.e., the direction of the velocity and the age of the star at the ejection) are fixed.
- The **axis ratio**, q_z, changes in each simulation.

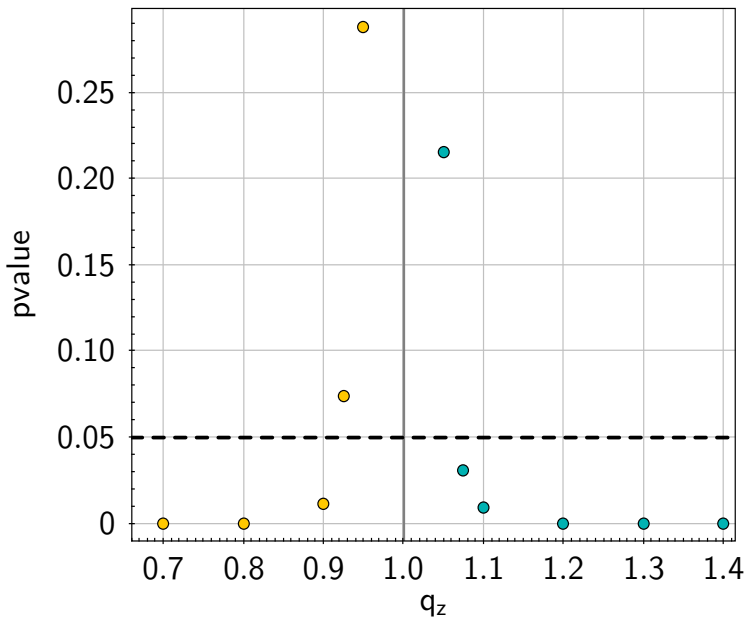

AG et al. (in prep.)

Randomizing the initial conditions

$\Rightarrow$ the smallest deviation from the spherical shape ($q_z = 1$) that can be significantly detected ($\mathrm{p-value} < 5\%$) varies from simulation to simulation.

Statistical analysis

Under the null hypothesis, the p – value is uniformly distributed over the interval [0,1].

$\Rightarrow$ Cumulative distribution: $f(x) = x$;

Procedure:

1) Generate a high number of mock catalogs for different q_z values

$\Rightarrow$ 5000 mock catalogs: $q_z = 0.7,\ 0.8,\ 0.9,\ 1,\ 1.1,\ 1.25,\ 1.4$

2) Compare them with 1 mock catalog generated in a given gravitational potential

$\Rightarrow$ 1 mock sample generated in a spherical DM halo.

Statistical analysis

3) Obtain a p − value distribution for each shape of the DM halo:

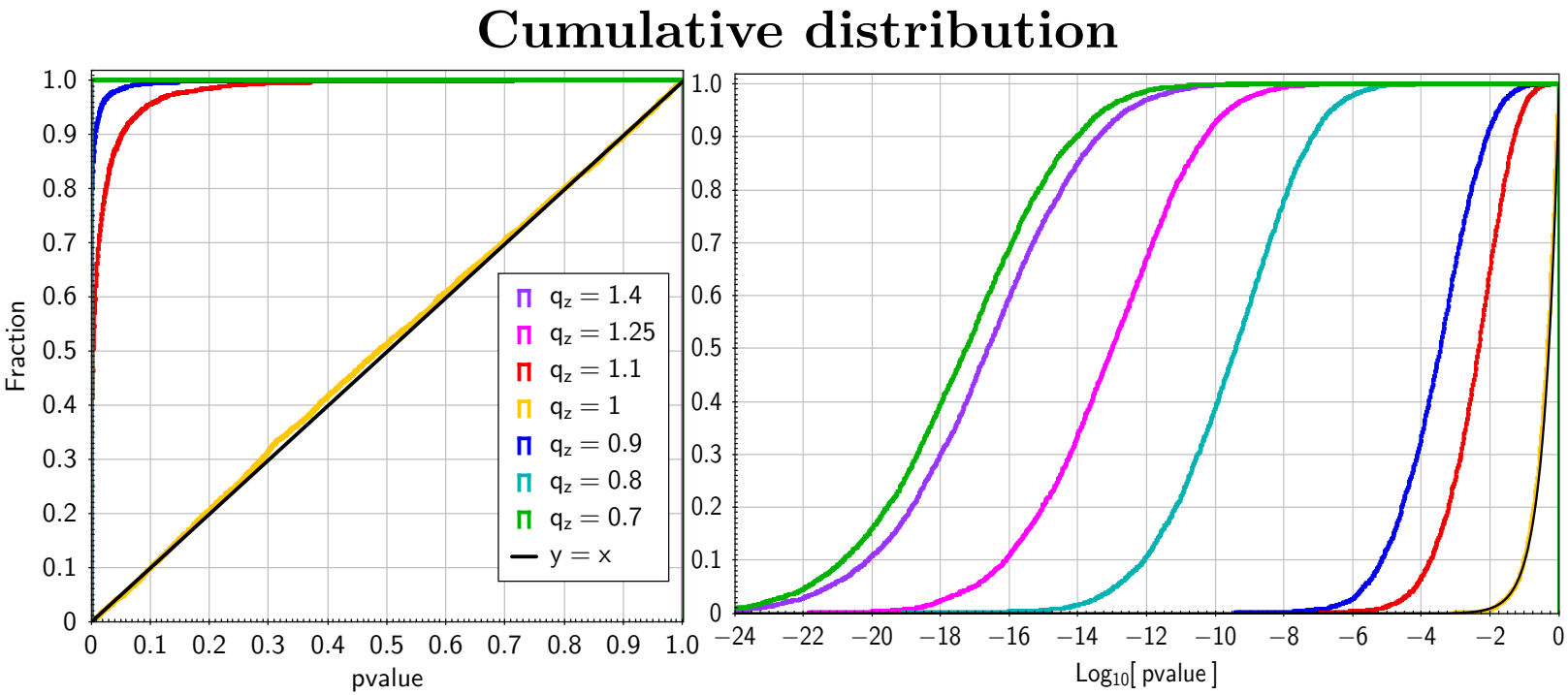

AG et al. (in prep.)

4) The q_z for which the cumulative distribution increases linearly is the one compatible with our "observed" sample.

Next steps

1) **Theoretical project**

a) Fully **triaxial DM halo** case:

$\Rightarrow$ $v_\theta^{\rm GC}$ & $v_\phi^{\rm GC}$ affected by the DM halo shape (loss of axial symmetry);

$\Rightarrow$ use of the **2-D K-S test**.

b) Effect of the observational uncertainties on the Galactocentric tangential velocities:

$\Rightarrow$ quantify the **proper motion precision** that is needed to distinguish among different halo shapes.

Next steps

2) **Observational project**

In collaboration with INAF-Osservatorio Astrofisico di Torino, we plan to:

a) identify new HVS candidates in the Galactic halo in the Gaia (E)DR3;

b) compare the kinematic properties of this sample with that of our mock catalogs in order to constrain the DM halo geometry.

Thanks for your attention!

Bibliography I

Hills, J. G., 1988, *Nature*, 331, 687

Brown, W. R. et al., 2005, *ApJ*, 622, L33

Rubin, V. C. & Ford, W. K. 1970, *ApJ*, 159

Ostriker, J. P. & Peebles, P. J. E., 1973, *ApJ*, 186, 467

Vera-Ciro, C. A. et al., 2011, *MNRAS*, 416, 1377

Zemp, M. et al., 2012, *ApJ*, 748, 54

Ibata, R. et al., 2001, *Nature*, 412, 49

Helmi, A., 2004, *ApJ*, 610, L97

Loebman, S. R. et al., 2014, *ApJ*, 794, 151

Law, D. R. & Majewski, S. R., 2010, *ApJ*, 714, 229

Gnedin, O. Y. et al., 2005, *ApJ*, 634, 344

Fragione, G. & Loeb, A., 2017, *New Astronomy*, 55, 3238

Bibliography II

- Contigiani, O. et al., 2019, *MNRAS*, 487, 4025
- Genzel, R. et al., 2010, *Reviews of Modern Physics*, 82, 3121
- Hernquist, L., 1990, *ApJ*, 356, 359
- Miyamoto, M. & Nagai, R., 1975, *PASJ*, 27, 533
- Navarro, J. F. et al., 1996, *ApJ*, 462, 563
- Vogelsberger, M. et al., 2008, *MNRAS*, 385, 236
- Ginsburg,I. & Loeb, A., 2006, *MNRAS*, 368, 221
- Zhang, F. et al., 2013, *ApJ*, 768, 153
- O'Leary, R. M. & Loeb, A., 2008, *MNRAS*, 383, 86
- Yu, Q. & Tremaine, S., 2003, *ApJ*, 599, 1129
- Wang, Y. et al., 2018, *MNRAS*, 475, 4595

S-stars

S-stars are stars orbiting around Sgr A* with highly eccentric orbit.
⇒ How did these stars obtain their highly eccentric orbits near the central SMBH?

In their studies of 2006, Ginsburg & Loeb simulated the orbits of the companion stars of HVSs.

→ Typically kicked into a highly eccentric orbit with an eccentricity similar to that observed for the S-stars.

This suggests a possible binary origin for these stars.

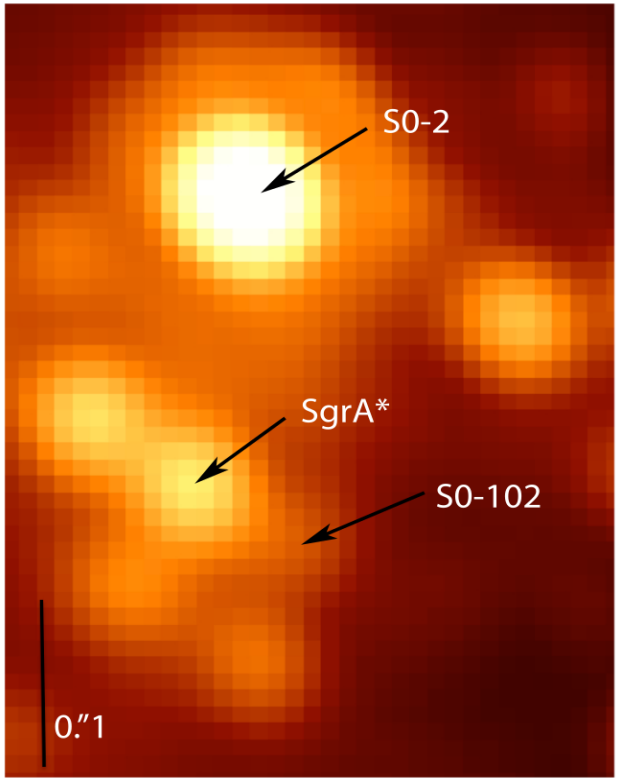

Hills velocity distribution: parameter sampling

The parameter sampling is performed as follows:

- the stellar binary semi-major axis, **a**, is randomly chosen according with the probability density function:

$$\mathrm{p(a)\,da} \sim \frac{\mathrm{da}}{\mathrm{a}} \ ,$$

  in the range $0.05\ \mathrm{AU} \leq a \leq 4\ \mathrm{AU}$;

- the minimum approach distance, **b**, is randomly chosen in the range [1 AU; 700 AU] according with the probability density function:

$$\mathrm{p(b)\,db} \sim \mathrm{b\,db} \ ;$$

Hills velocity distribution: parameter sampling

The **probability** density function of the semi-major axis is given from observations of large samples of stellar binary systems.

The **range** of values is motivated by:

$\Rightarrow$ $\underline{a < 0.05\ \mathrm{AU}}$: ejections only for very small b values, that likely produce a tidal disruption event rather than a HVS;

$\Rightarrow$ $\underline{a > 4\ \mathrm{AU}}$: very low ejection velocities $\rightarrow$ stars are very unlikely to reach the Galactic halo.

Hills velocity distribution: parameter sampling

The **probability** density function of closest approach distances, b, to Sgr A* is the result of the gravitational focusing.

$\Rightarrow$ the enhancement in the likelihood that two particles will collide, due to their mutual gravitational attraction.

The **range** of values is motivated by:

$\Rightarrow$ $\underline{\mathrm{b} < 1\ \mathrm{AU}}$: tidal disruption events;

$\Rightarrow$ $\underline{\mathrm{b} > 700\ \mathrm{AU}}$: no ejection, the value of 700 AU correspond to the value that gives a zero ejection probability when $\mathrm{a} = 4$ AU.

Hills velocity distribution: parameter sampling

The parameter sampling is performed as follows:

- the inclination angle, **i**, between the binary revolution plane and the orbital plane of the center of mass around the SMBH, is randomly sampled in the interval $[0, 2\pi]$ with a uniform probability density function;
- the initial phase, ϕ of the binary is randomly sampled in the interval $[0, 2\pi]$ with a uniform probability density function;

Star ejection

The star ejection takes place when the SMBH tidally disrupts a stellar binary.

The code checks if the binary has been disrupted or not:
$\Rightarrow$ if the binary total energy in the CM reference frame, E_{bin}, is positive, the binary has been disrupted.

$$E_{bin} = \frac{1}{4} M_\star \sum_i (\Delta v_i)^2 - \frac{G M_\star}{a},$$

where Δv_i is the difference between the i-th velocity component of the two stars.

Star ejection

Then the code decides which star has been ejected:

$\Rightarrow$ the total energy of both stars is calculated in the SMBH reference frame and the star with positive energy is the ejected one.

The velocity at infinite distance from the SMBH is computed starting from total energy conservation and is:

$$v_{ej} = \sqrt{v_\star^2 - \frac{2G\mathrm{M_{SMBH}}}{b}},$$

where:

$$v_\star = \sqrt{\frac{GM_\star}{2a}}.$$

Gravitational potential

Model parameters:

M_{BH} [$M_\odot$]	M_b [$M_\odot$]	r_b [kpc]	M_d [$M_\odot$]	a_d [kpc]	b_d [kpc]	M_{200} [$M_\odot$]	r_s [kpc]	C_{200}
4×10^6	3.4×10^{10}	0.7	10^{11}	6.5	0.26	8.35×10^{11}	18	10.82

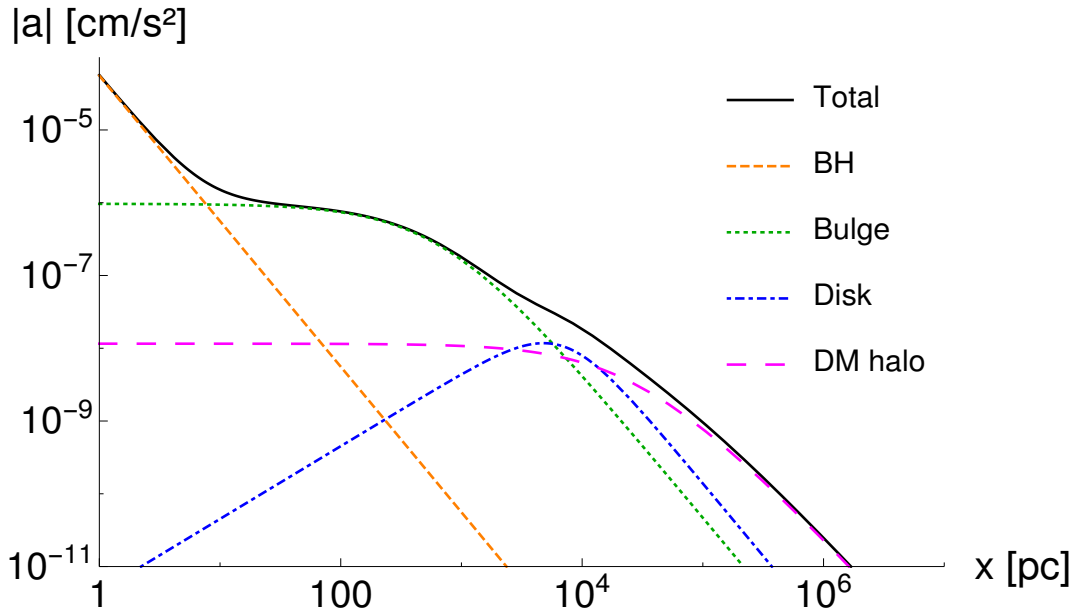

AG et al. (in prep.)

The times

$$N(t) = R\,(t_{ms} - t_{age})\,(1 - e^{-\frac{t}{t_{ms}-t_{age}}}) \;\Rightarrow\; \lim_{t\to\infty} N(t) = R\,(t_{ms} - t_{age})$$

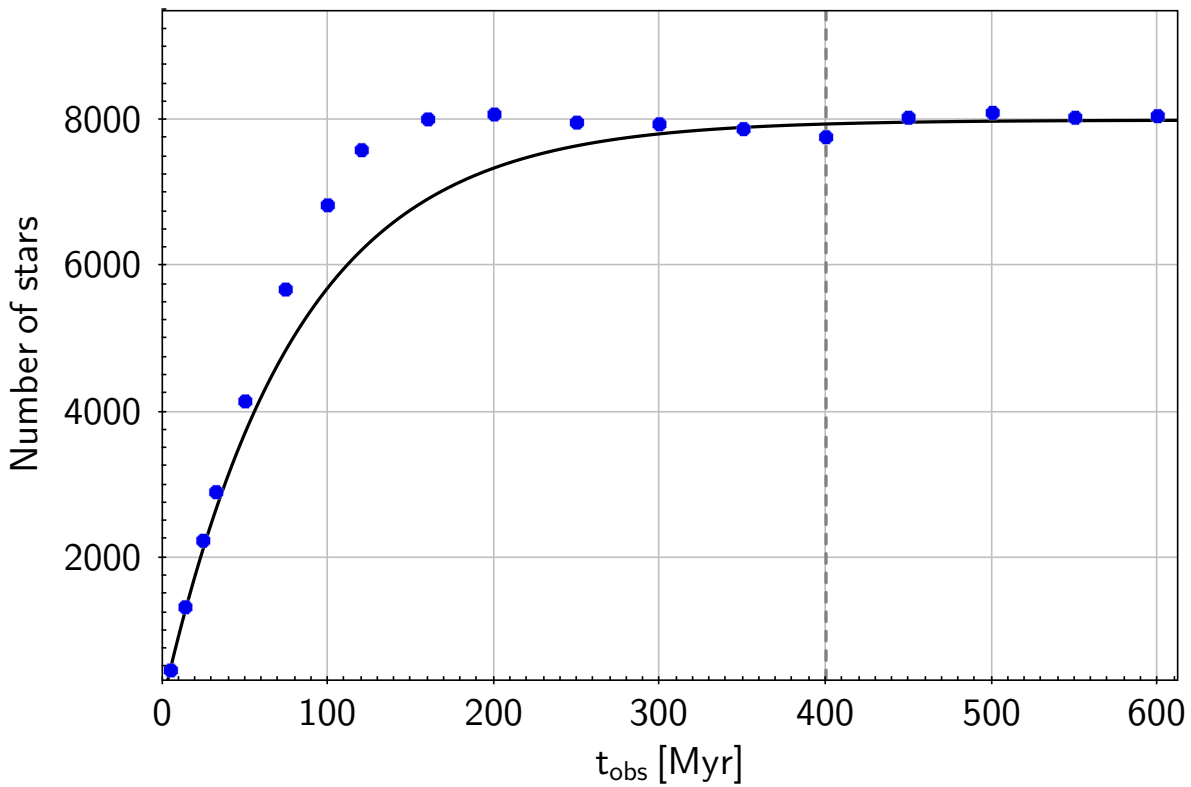

AG et al. (in prep.)

Sample selection

For stars with low ejection velocities ($v_{\rm ej} \lesssim 700$ km/s), angular velocities are tightly coupled with the radial velocity.

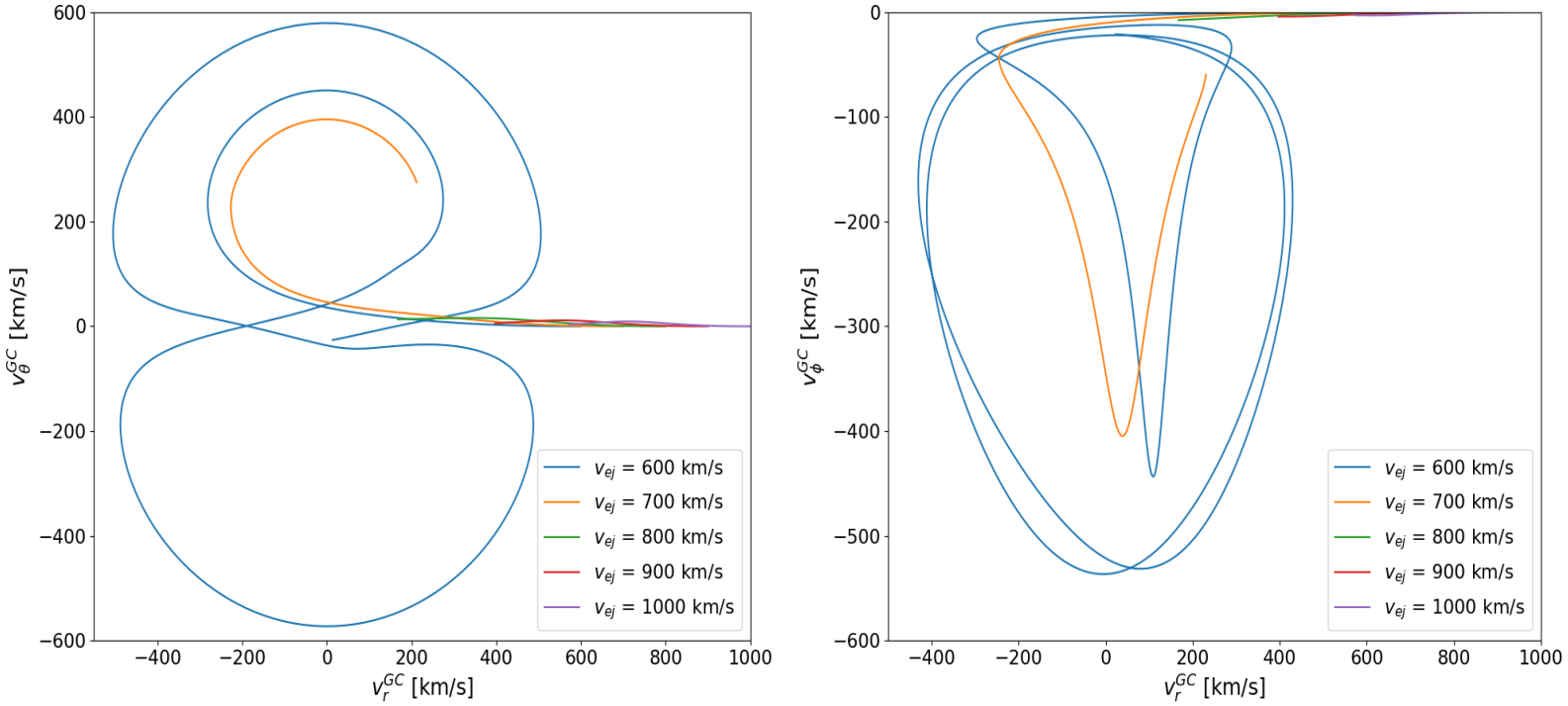

Figures: Left panel: $q_y = 1$, $q_z = 1$; right panel: $q_y = 0.8$, $q_z = 1$.

AG et al. (in prep.)

Sample selection

We select only the stars that at t_{obs}:

1) $r^{\rm GC} \geq 10$ kpc; 2) $v_r^{\rm GC} > 0$ km/s;

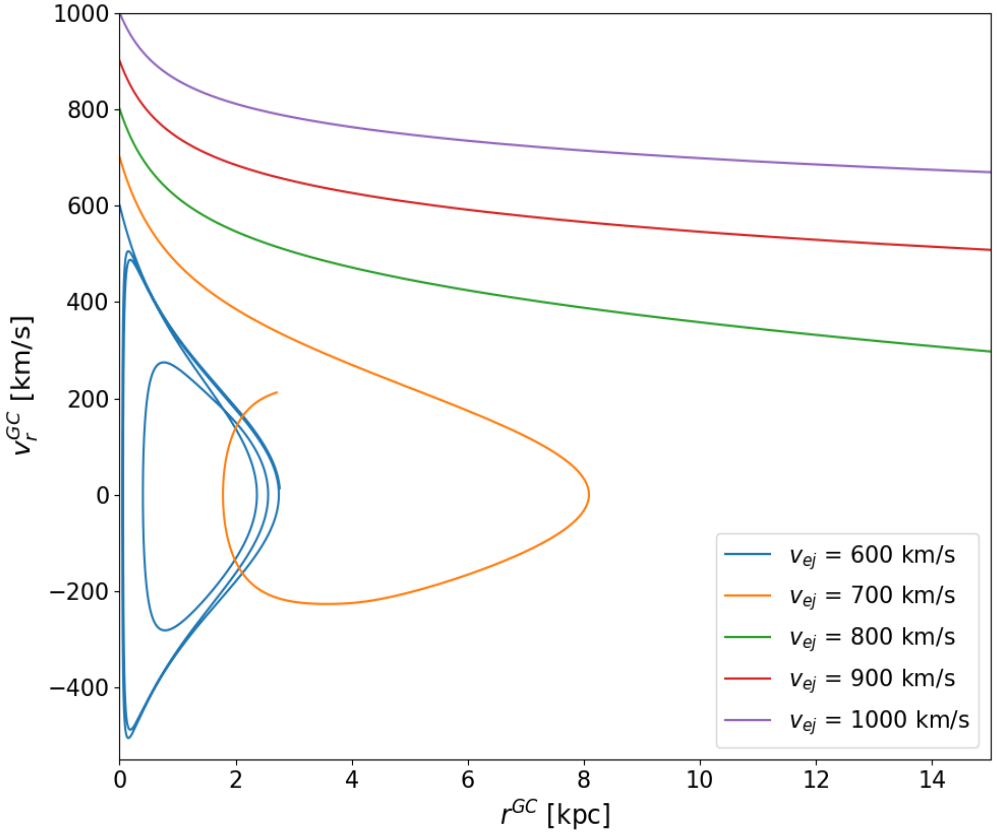

AG et al. (in prep.)

Relevant timescales

Rate of ejection: $\mathrm{R} = 10^2 \, \frac{\mathrm{stars}}{\mathrm{Myr}}$ (Zhang et al. 2013).

Ejection time: t_{ej}, uniformly chosen between 0 Myr and t_{max}.

Observation time: t_{obs}, fixed and equal for each star.

Travel time: $t_{travel} = t_{obs} - t_{ej}$.

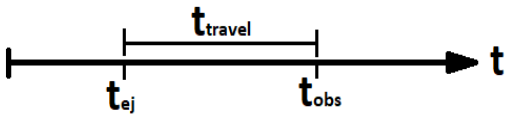

Main-sequence lifetime: $t_{ms} = 160\,\mathrm{Myr}$, for a $4\,\mathrm{M}_\odot$ star.

Age of the star: t_{age}, uniformly sampled between 0 and t_{ms}.

$\Rightarrow$ $t_{age} + t_{travel} > t_{ms}$ $\rightarrow$ the star is rejected;

$\Rightarrow$ $t_{age} + t_{travel} < t_{ms}$ $\rightarrow$ the star trajectory is computed.

Alternative mechanisms

- 3-body interactions of stars with a stellar mass black hole (SBH) orbiting a SMBH (O'Leary & Loeb 2008).
- 3-body interactions of stars with a binary SMBH can eject single stars as HVSs (Yu & Tremaine 2003);
- 4-body interactions of stellar binaries with a SMBH binary system can eject both single and binary HVSs (Wang et al. 2018).

Wang's mechanism

Wang's mechanism
A binary BH system in the center of a galaxy:

- SMBH,
- IMBH,

can eject the stars of the stellar binaries in its proximity.

Recent observational constraints on the Galactic BBH:

- $M_{\rm SMBH} = 4 \times 10^6 {\rm M}_\odot$;
- $M_{\rm IMBH} = 10^4 {\rm M}_\odot$, at $r_{\rm GC} = 0.13\,{\rm pc}$. (Tsuboi et al. 2017)

Wang's mechanism

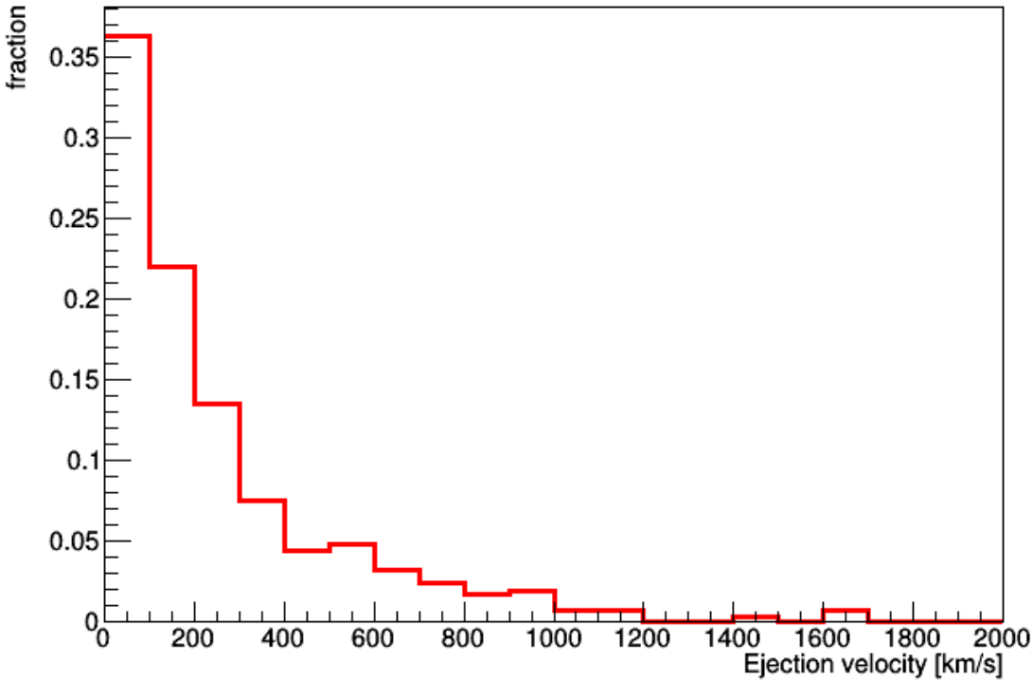

S. Ebagezio, L. Ostorero, **AG**, (in prep.)

Aim of the project:
testing the goodness of the Wang's mechanism in explain HVSs current observations, given the density of stars near the Galactic center.